V European Conference on Computational Fluid Dynamics
ECCOMAS CFD 2010
J. C. F. Pereira and A. Sequeira (Eds)
Lisbon, Portugal,14-17 June 2010

NUMERICAL STUDY OF THERMOACOUSTIC WAVE AMPLIFICATION

Catherine Weisman[*†], Diana Baltean Carlès[*†], Patrick Le Quéré[*] and Luc Bauwens[‡]

[*]Laboratoire d'Informatique pour la Mécanique et les Sciences de l'Ingénieur, LIMSI-CNRS UPR3251,
BP 133, F-91403 Orsay France
e-mail: weisman@limsi.fr
[†]Université Pierre et Marie Curie
4 Place Jussieu, 75252 Paris Cedex 05, France
[‡]University of Calgary, Department of Mechanical and Manufacturing Engineering
2500 University Drive NW, Calgary, AB T2N 1N4, Canada
e-mail: bauwens@ucalgary.ca

Key words: Fluid Dynamics, Acoustics, Thermoacoustics, Multiple scale

Abstract. *Heat exchanger configuration, including unavoidable dead space, affects the performance of thermoacoustic devices. Three different models are compared numerically: ideal heat exchangers, modeled as a fluid zone where temperature is prescribed at all times, hot for the heater and cold for the cooler, and two more realistic arrangements, in which the heat exchangers are made up of horizontal plates with a prescribed blockage ratio. In one of these, a fixed temperature is imposed in the heat exchanger plates, while in the other, constant heat fluxes are prescribed. The thermoacoustic engine consists of a stack and heat exchangers, placed inside a long tube closed at one end and equipped with a load at the other end. It is modeled coupling a numerical simulation of the viscous and conducting flow in the stack and heat exchangers with linear acoustics in the left and right parts of the tube (the resonators), based upon multiple scale analysis. When a sufficiently large temperature difference is applied between the heat exchangers, initial pressure perturbations are amplified, the fluid starts oscillating and amplitudes grow, up to the point when the engine reaches a stationary periodic operation. The three heat exchanger models result in a similar behavior. The initial amplification is a function of the initial temperature gradient along the stack plates. However, the presence of a small void volume between heat exchangers and stack considerably lowers the initial temperature gradient in the stack. Different resonating modes are amplified depending upon the configuration, which is in agreement with experimental observations.*

1 INTRODUCTION

The main attraction of thermoacoustic engine is absence of any moving part. The standing wave engine consists of a long resonating tube, closed at one end, and with a load placed at the other end. A stack, usually made up of parallel plates, is placed inside the resonator. One extremity of the stack is maintained at a hot temperature while the other end is kept cold; to that effect, heat exchangers are required on both sides. The combination of pressure fluctuation and oscillating heat exchange in the boundary layers along the plates results in a heat engine effect [1, 2, 3]. However, design and construction of the heat exchangers is challenging; usually there remains a dead space filled with cycle fluid between the heat exchangers and the end of the stack. Here, engines with different heat exchanger models and configurations are compared and the effect of these dead spaces is quantified.

The model used includes a direct simulation of the viscous, conducting flow in the stack and heat exchangers, coupled with an exact solution of linear acoustics in the resonators. In a properly designed device in stationary operation, the flow should sweep a length comparable with the stack length, while to avoid large losses in the resonators the Mach number should remain low. Thus it is reasonable to assume that the flow is low Mach number, and that the length of the stack+heat exchangers section is of the order of the total length times the Mach number. The low Mach number flow in the resonator is then characterized by length and time scales in a ratio of the other of the speed of sound, while in the heat exchangers, length and time are in a ratio of the order of the fluid velocities, yielding respectively and acoustic flow and a dynamically incompressible flow. Pressure fluctuations are restricted to an acoustic amplitude by the flow in the resonators. Matching these two solutions in the standard way provides appropriate boundary conditions to the heat exchanger flow problem which is solved numerically. From the standpoint of resonator acoustics, the heat exchangers are transparent to pressure but they provide a source of volume. For details on the multiple scale model, see [4, 5].

2 PHYSICAL MODEL AND MULTIPLE SCALE FORMULATION

The geometry consists of a long tube with length L_R, within which a set of heat exchangers with characteristic length L_S is placed, at a location $x = 0$. The stack consists of a set of parallel plates. It is assumed that the heater and the cooler have the same periodicity so that the simulation can be reduced to a domain consisting of two half-plates plus the gap between them, and a consistent fraction of the resonator cross-section. The geometry of the heat exchanger section (the simulation domain) is shown in Fig. 1. One resonator end, located at x_L is closed, while the second consists of a load. The latter, for instance a piston, entails some motion of the tube end; however that motion is of the order of the particle displacement hence small compared with the tube length. Thus the load is readily reduced to an impedance at a fixed location x_R.

The multiple scale formulation has been described in detail elsewhere [4, 5]. A brief

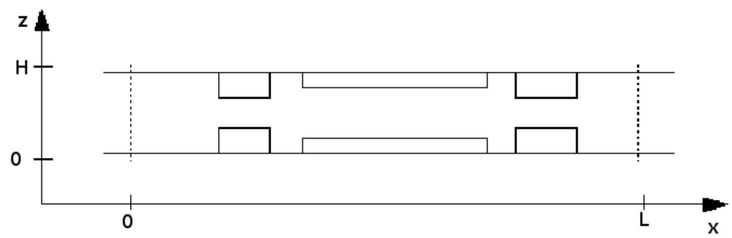

Figure 1: Stack and heat exchanger geometry

overview follows. The key scaling assumptions made are that at the stationary regime, velocities are small compared with the speed of sound, and that they span a length of the order of the length of the stack or heat exchanger section. Then since for an acoustic resonance, the resonator length is of the order of the speed of sound times the period, while the length of the heat exchangers is like the velocity times the period, the ratio between the characteristic length L_S and the resonator length L_R equals the reference Mach number M. Assuming a time scale of the order of the period, velocities corresponding to the reference Mach number, and these respective length scales, flow in the resonator is characterized by a linear acoustic problem. Flow in the heat exchangers however is described by a dynamically incompressible model, with order M^2 pressure gradients superimposed to spatially uniform pressure fluctuations, potentially up to leading order; however continuity of pressure between the two solutions limits these spatially uniform to the magnitude of the fluctuations in the resonators, which are of order M.

Without loss of generality (i.e. avoiding any assumption on the shape of the waves, and avoiding a Fourier representation), acoustics in the two parts of the resonator can be expressed as a d'Alembert solution, as a pair of traveling waves that move respectively left and right at the speed of sound with no interaction except at boundaries. At the two tube ends, however, the boundary conditions result in a relationship that determines the outgoing wave as a function of the incoming wave (a model often described as a "reflection coefficient"). In the current context, this model reduces resonator acoustics to boundary conditions, on both sides of the heat exchanger sections, relating order M pressure and velocity to their values at a previous time equal to the round trip time between heat exchanger location and the respective end at the respective speed of sound.

Under the scaling above, at leading order and at order M, the momentum equation is reduced respectively to $\nabla p^{(0)} = 0$ and $\nabla p^{(1)} = 0$, in which the superscript characterizes the magnitude of the pressure contribution in a Taylor expansion in the reference Mach number M. The resulting problem includes momentum at order M^2 together with the leading order conservation laws for mass and energy:

$$\frac{\partial \rho}{\partial t} + \nabla.(\rho \mathbf{u}) \quad = \quad 0$$

$$
\begin{aligned}
\frac{\partial(\rho\mathbf{u})}{\partial t} + \nabla.(\rho\mathbf{u}\otimes\mathbf{u}) &= -\nabla p^{(2)} + \frac{1}{Re}\nabla.\tau \\
\rho\left[\frac{\partial T}{\partial t} + (\mathbf{u}.\nabla)T\right] &= \frac{1}{Pe}\nabla^2 T
\end{aligned}
\tag{1}
$$

in which it has already been taken into account that, scaling the thermodynamic properties by reference values, $p^{(0)} = \rho T = 1$. The stress tensor $\tau = [\nabla\mathbf{u} + (\nabla\mathbf{u})^t - \frac{2}{3}(\nabla.\mathbf{u})\mathbf{I}]$, the reference Reynolds number is evaluated based upon the reference velocity, L_S and viscosity at the reference state and likewise for the reference Péclet number. In the solid plates (either the stack plates or the heat exchanger plates) the dimensionless heat conduction equation is:

$$
\frac{\partial T}{\partial t} = \frac{1}{Pe_s}\Delta T, \tag{2}
$$

where the solid Péclet number is defined as $Pe_s = Pe\alpha_{ref}/\alpha_s$, α_{ref} and α_s being thermal diffusivities respectively at the reference state in the fluid and in the solid, with the latter depending upon the solid material.

In the limit of $M \to 0$, in the outer scaling, associated with the resonator and with acoustics, the length of the stack and heat exchangers $\to 0$. In the inner scaling, associated with the stack and heat exchangers, the resonators become infinitely long. Matching the two problems requires values of pressure and velocity to approach the same limits. Given that in the heat exchangers, $\nabla p^{(1)} = 0$, these are in effect transparent to acoustic pressure, which is thus continuous between the two sides of the resonator. However for velocity, integration of the energy equation over the heat exchangers and stack (including additional lengths on both sides that $\to \infty$) yields

$$
(u_L - u_R)H + \frac{1}{Pe}\int \nabla T \cdot \mathbf{n} ds = 0 \tag{3}
$$

in which H is the height of the simulation domain. Continuity of $p^{(1)}$, together with the acoustic boundary conditions on both sides, at the heat exchanger location, and Eq. (3) provide three equations for the three unknowns $p^{(1)}$, u_L and u_R. Solving provides closure to the acoustic problem, and boundary conditions to the problem in the stack and heat exchangers, which is then solved numerically.

3 NUMERICAL SOLUTION

The problem in the heat exchangers and stack is solved numerically using a code originally developed to deal with non-Boussinesq convection, hence suitable for density and temperatures that vary at leading order, and spatially uniform pressure fluctuations at up to leading order, both for velocities restricted to a small Mach number [6]. Diffusion is dealt with implicitly while advection is explicit. Both are second-order accurate in space and time. A fractional step projection method adapted for variable density is used to enforce continuity. Both the ADI and GMRES algorithm have been tested to solve the

Helmholtz equation for temperature and velocities. A multigrid algorithm determines the pressure correction.

Solution of the coupled equations providing velocity boundary conditions from resonator acoustic are appropriately integrated in the solution sequence. An extensive validation of the current implementation has been performed with satisfactory results [4, 5].

4 RESULTS

Results were obtained for a device geometry studied by Atchley et al. [7], 1 m long, with a 3.5 cm long stack, using helium, for various mean pressure values. Since $L_R/L_S = 28.6$, $M = 0.035$. The heat exchangers are placed at a distance of $0.055L_R$ from the left (closed) end. As to widths, there are respectively 0.0222 L_S and 0.008 L_S for the stack gap and the stack plate, which is made of stainless steel. Heat exchangers are made of nickel; they are 0.009 L_S thick; the hot heat exchanger is 0.21 L_S long and the cold one is 0.63 L_S, with passages 0.021 L_S wide. The distance between heat exchanger and stack is the same on both sides, equal to the stack gap.

For the heat exchangers, two configurations with geometry as shown in Fig. 1 were used, respectively assuming the entire heat exchanger wall to be at imposed heat exchanger temperatures, or imposing a longitudinally uniform heat flux along the outer heat exchanger boundaries (i.e. the symmetry lines that bound the simulation domain). The third model assumed ideal heat transfer, by forcing the fluid to adopt the imposed heat exchanger temperatures within transverse slices crossing the entire domain, as shown in Fig. 2.

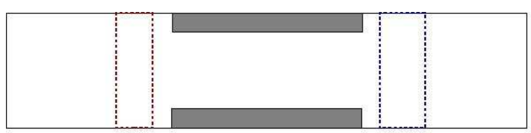

Figure 2: Ideal heat exchangers: in the regions delineated, fluid temperatures are imposed

Initial conditions considered fluid at rest and temperature profiles obtained numerically, corresponding to steady conduction solutions in the walls and in fluid at rest. Figure 3 shows the respective temperature fields close to the hot heat exchanger. Differences

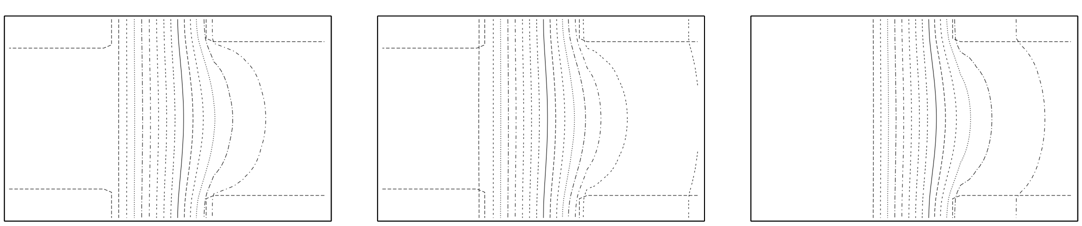

Figure 3: Initial temperatures. Left to right: imposed temperature, imposed heat flux, ideal exchangers

between the two realistic heat exchangers and the ideal one are perhaps more obvious in Fig. 4, which shows the difference in the initial profiles along the centerline. The effect of conduction in the gap on the temperature gradient in the stack is clear.

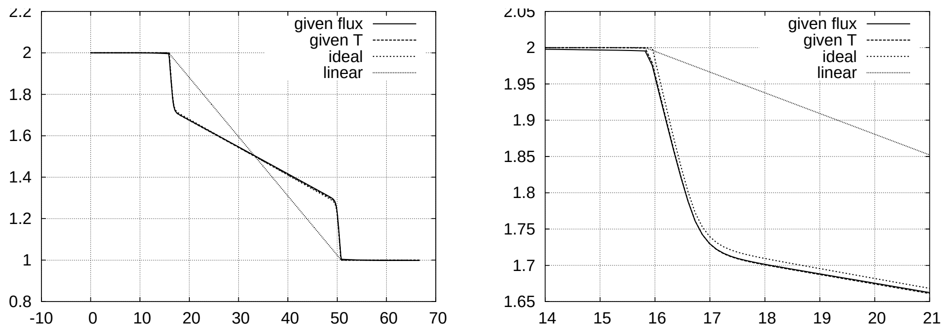

Figure 4: Initial temperatures along the centerline. Left: entire heat exchanger section. Right: near hot heat exchanger

Resolutions of 512 × 32, 1024 × 64 and 512 × 64 grid points were used, with about 1000 time steps/period, until velocity increased and then the step size was decreased by a factor ten. Convergence was found to be satisfactory. ADI and GMRES yielded indistinguishable results; being faster, the former was used for the results below.

First, results for three different values of the mean pressure were compared, all for heat exchangers at fixed temperatures. Results describing the early part of the amplification process are shown in Figs. 5 to 7, all for a hot heat exchanger 450 K above the cold one.

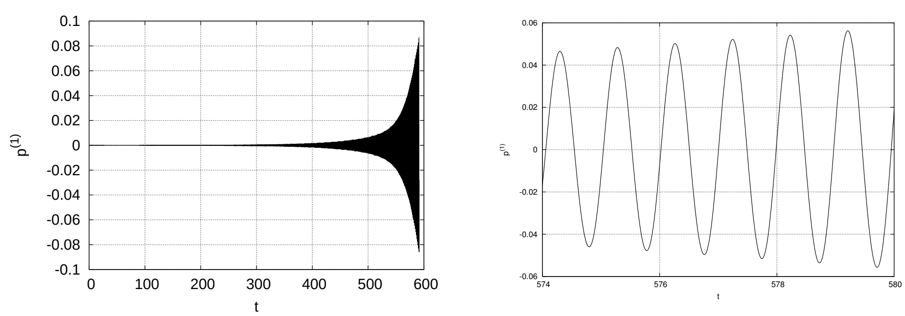

Figure 5: Acoustic pressure. Left, time history. Right, detail over narrow window. $\tilde{p}_{ref} = 150kPa$

Because these results were obtained for different loads, that some results show the thermoacoustic instability taking longer to manifest itself and grow does not lend to any meaningful conclusion. However, there is also a mode switch. At higher pressure, the dimensionless period is close to the fundamental in a tube at ambient temperature, with value equal to 2.0 in the current scaling. However when the pressure is reduced the first harmonic, with period close to unity, is being amplified at the lowest pressure. Finally, for

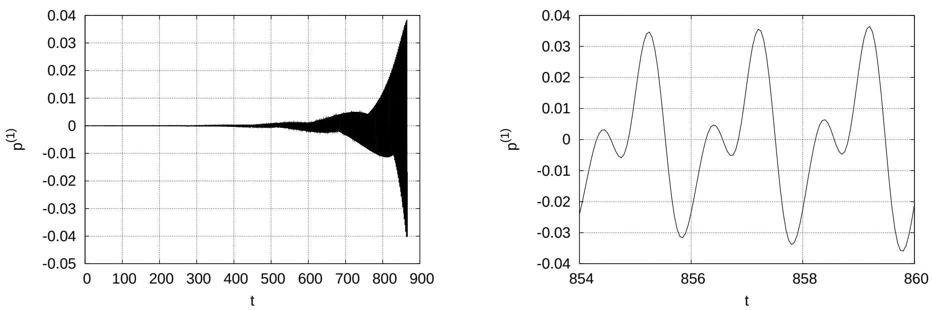

Figure 6: Acoustic pressure. Left, time history. Right, detail over narrow window. $\tilde{p}_{ref} = 240kPa$

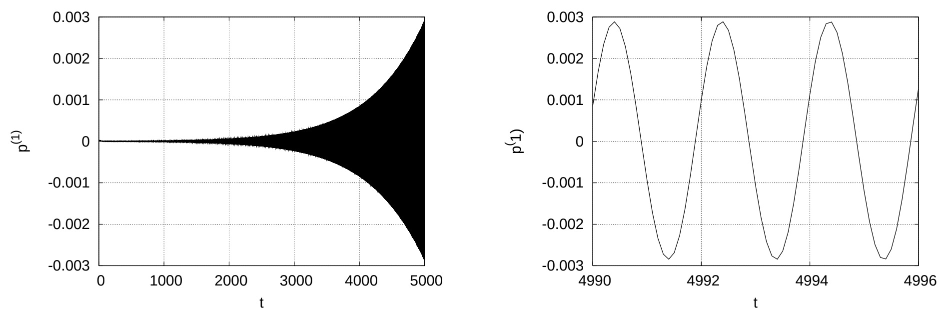

Figure 7: Acoustic pressure. Left, time history. Right, detail over narrow window. $\tilde{p}_{ref} = 440kPa$

an intermediate value, initially the fundamental appears, but eventually the first harmonic becomes dominant. These results are consistent with [7].

Results for different heat exchanger models are shown in Figs. 8 and 9, for a temperature difference of 450 K, except for Fig 9, and a load characterized by an impedance $f = p^{(1)}/u = 100$. Results for realistic heat exchangers, either with imposed temperatures, or heat fluxes, are indistinguishable.

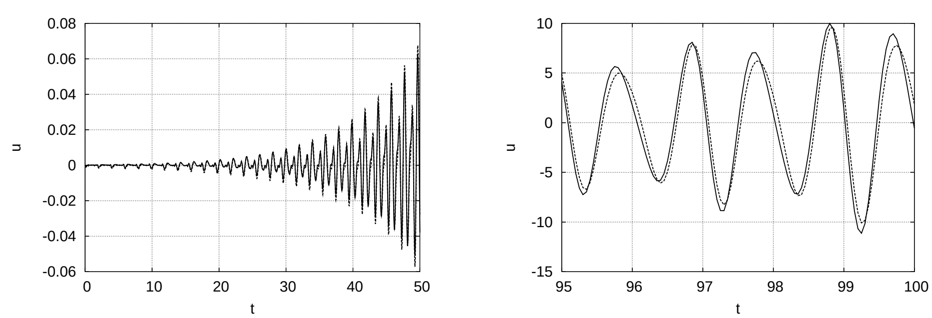

Figure 8: Longitudinal velocity, right side of the heat exchanger section. Left, time history. Right, narrow window. Solid curve for realistic exchangers, dashed line for ideal ones. Mean pressure 150 kPa

Next the effect of the load was examined. Figures 10 and 11 show the influence of the load, all for a pressure of 440 kPa and a temperature difference of 262 K, for realistic heat exchangers at prescribed temperature.

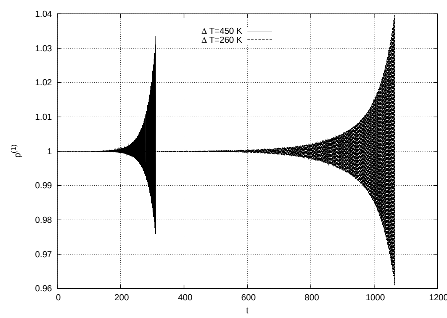

Figure 9: Acoustic pressure for temperature differences of 260 K and 450 K. Mean pressure 440 kPa

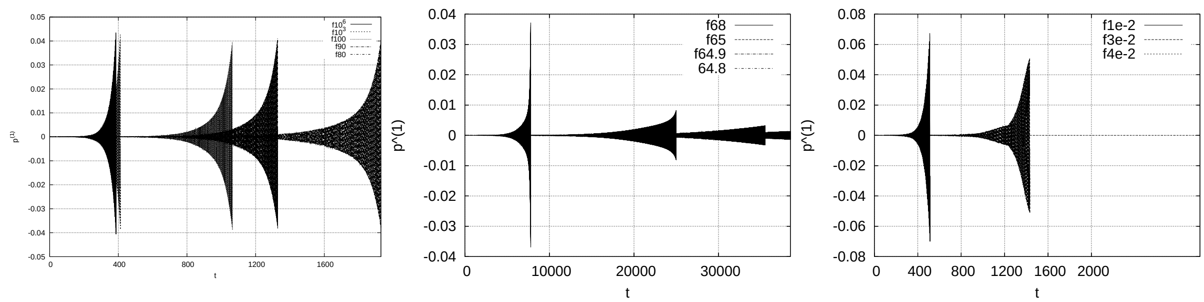

Figure 10: Acoustic pressure for $f = 10^6$, 10^3, 100, 90 and 80 (left); $f = 68$, 65, 64.9 and 64.8 (middle); $f = 0.04$ and 0.02 (right)

These results show that initially, as the load impedance decreases, the instability takes longer to grow. However, for a value in the neighborhood of 55, the trend switches direction, and further decrease of the impedance leads to an instability that is developing earlier. This is consistent with existence of an impedance that maximizes the power developed by the engine. Indeed, power becomes zero for both an infinite and a zero impedance, hence existence of a maximum for an intermediate value. It is clear that the power absorbed by the load reduces the power left for amplitude growth. As shown in Fig. 11, for very low impedance, the frequency doubles. This is consistent with a zero impedance representing an open end, which leads to resonant modes with a frequency double that for an open end in straight tubes with uniform temperature.

5 CONCLUSION

Direct simulation of a complete thermoacoustic engine was performed. Based upon a multiple scale analysis, the global compressible flow problem is reduced to a dynamically incompressible problem in the heat exchangers, with boundary conditions derived from linear acoustics in the resonator.

The model was used to study several features of the engine, such as influence of load impedance, temperature differences, mean pressure and heat exchanger models. Results show that the approach will yield valuable information on the operation of the engine, which remains otherwise rather opaque. While simulations remain relatively large, as the

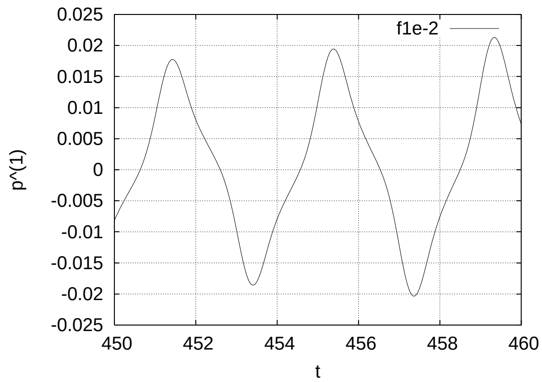

Figure 11: Acoustic pressure - detail for $f = 0.02$

current results show, it is possible to use the model in parametric study, which will help understanding tradeoffs.

ACKNOWLEDGMENTS

Support of the Natural Sciences and Engineering Research Council of Canada is gratefully acknowledged (LB).

Computations were performed on the NEC-SX8 of the IDRIS-CNRS computing center, under project No. i2009020599.

REFERENCES

[1] N. Rott, Damped and thermally driven acoustic oscillations in wide and narrow tubes, *Z. Angew. Math. Phys.*, **20**, 230–243 (1969).

[2] G.W. Swift, Thermoacoustic engines, *J. Acoust. Soc. Am.*, **84**, 1145–1180 (1988).

[3] L. Bauwens, Oscillating flow of a heat-conducting fluid in a narrow tube, *J. Fluid. Mech.*, **324**, 135–161 (1996).

[4] O. Hireche, C. Weisman, D. Baltean Carlès, P. Le Quéré, M. X. François and L. Bauwens, Numerical Model of a Thermoacoustic Engine, *Comptes rendus Mécanique*, **338**, 18–23 (2010).

[5] O. Hireche, C. Weisman, D. Baltean Carlès, P. Le Quéré and L. Bauwens, Multiple Scale Analysis and Simulation of Thermoacoustic Engines, *J. Acoust. Soc. Am.*, in press.

[6] P. Le Quéré, R. Masson and P. Perrot, Chebyshev collocation algorithm for 2D non-Boussinesq convection, *J. Comp. Physics*, **103**, 320–335 (1992).

[7] A.A Atchley and F. M. Kuo, Stability curves for a thermoacoustic prime mover, *J. Acoust. Soc. Am.* **95**, 1401–1404 (1994).